1   **Selection-free non-viral method revealed highly efficient CRISPR-Cas9 genome**
2   **editing of human pluripotent stem cells guided by cellular autophagy**
3

4   Michelle Surma[1], Kavitha Anbarasu[1,2] and Arupratan Das[1,2,3,4,5,*]
5

6   [1]Department of Ophthalmology, Eugene and Marilyn Glick Eye Institute, Indiana
7   University, Indianapolis, IN 46202, USA; [2]Department of Medical and Molecular
8   Genetics, Indiana University, Indianapolis, IN 46202, USA; [3]Stark Neurosciences
9   Research Institute, Indiana University, Indianapolis, IN 46202, USA; [4]Department of
10 Biochemistry and Molecular Biology, Indiana University, Indianapolis, IN 46202, USA
11
12 [5]Lead Contact
13 *Correspondence: arupdas@iu.edu
14

15 **SUMMARY**

16

17 CRISPR-Cas9 mediated genome editing of human pluripotent stem cells (hPSCs)

18 provides strong avenues for human disease modeling, drug discovery and cell

19 replacement therapy. Genome editing of hPSCs is an extremely inefficient process and

20 requires complex gene delivery and selection methods to improve edit efficiency which

21 are not ideal for clinical applications. Here, we have shown a selection free simple

22 lipofectamine based transfection method where a single plasmid encoding guide RNA

23 (gRNA) and Cas9 selectively transfected hPSCs at the colony edges. Upon dissection

24 and sequencing, the edge cells showed more than 30% edit frequency compared to the

25 reported 3% rate under no selections. Increased cellular health of the edge cells as

26 revealed by reduced autophagy gene-expressions is critical for such transfection pattern.

27 Edge specific transfection was inhibited by blocking lysosomal activity which is essential

28 for autophagy. Hence, our method provides robust scarless genome-editing of hPSCs

29 which is ideal for translational research.

30

31   **INTRODUCTION**

32

33   Genome editing of hPSCs by CRISPR-Cas9 provides many unprecedented advantages,

34   from introducing disease specific gene deletions to precise DNA base pair changes.

35   Genome edited hPSCs are differentiated to the human cell of interest for disease

36   modeling, drug screening, or cell replacement therapy, with potential use for personalized

37   medicine (Saha and Jaenisch, 2009). Successful delivery of Cas9 gene and gRNA

38   specific to the target gene is critical for gene editing in hPSCs. However, CRISPR-Cas9

39   mediated genome editing of hPSCs is an extremely inefficient process with success rate

40   less than 3% (Yang et al., 2013). To increase genome-editing efficiency in hPSCs, several

41   approaches have been taken including: stable integration of a drug selection marker into

42   the genome (Lombardo et al., 2007), transient selection (Sluch et al., 2018; Steyer et al.,

43   2018), fluorescence-activated cell sorting (FACS) (Ding et al., 2013) and more recently a

44   combination of electroporation and viral transduction based methods (Martin et al., 2019).

45   While these methods have improved genome editing efficiency, they also possess

46   unwanted consequences, such as permanent gene alterations through integration of

47   selection markers which could disrupt the local transcriptional regulation and will make

48   hPSCs incompatible for clinical applications. FACS based single cell sorting to enrich

49   Cas9 expressing cells increased edit efficiency to 6.0% in hPSCs but with very low cell

50   survival rate (Byrne and Church, 2015; Yang et al., 2013). Viral gene delivery methods

51   require special skill in producing virus particles, which is a lengthy process and not ideal

52   for most laboratories. Antibiotic selection to enrich the transfected cells activates innate

53   immunity and genetic changes which are not ideal for downstream translational

2

54   applications (Mignon et al., 2015; Vandermeulen et al., 2011). Thus, there is a critical

55   need for developing a CRISPR-Cas9 mediated genome editing technique for hPSCs

56   without the need for any antibiotic selection, FACS sorting or complex viral transduction-

57   based methods.

58

59   To achieve this goal, here we first explored the differential transfection potential of stem

60   cells within a hPSC colony and have identified that cells at the colony edges selectively

61   got transfected due to increased cellular health compared to the cells at the center. Using

62   a single plasmid containing gRNA/Cas9 and lipofectamine based transfection, we found

63   very high Cas9 expression with more than 30% genome editing frequency through non-

64   homologous end joining (NHEJ) at the edge cells compared to the center. This simple but

65   highly efficient scarless genome editing technique of hPSCs is ideal for disease modeling

66   research and clinical applications.

67

68   **RESULTS**

69

70   **Cells at the hPSC colony edges are selectively transfected by plasmid DNA**

71

72   We used a simple lipofectamine-based transfection to hPSCs which requires only mixing

73   of the lipofectamine reagent and plasmid DNA containing Cas9/gRNA followed by

74   addition to the cells. To identify if hPSC culture shows any cellular pattern for transfection

75   which could be exploited to enrich the transfected cells, first we transfected H7 human

76   embryonic stem cells (H7-hESCs) by CAG-mCherry plasmid at the single cell level or at

77 the colony stage which is formed by compacting several cells. Much to our surprise, we

78 observed stem cells at the colony edge got selectively transfected but not cells the at

79 colony center (Figure 1A), while single cell culture got transfected randomly with no such

80 pattern (Figure 1B) as observed by the mCherry fluorescence. However, overall

81 transfected cell population showed no difference between the single cell and colony

82 stages when measured by flow cytometer (Figures 1C, 1D). To measure if stem cells at

83 the colony center are not expressing mCherry and hence not transfected, we drew a line

84 across the colony center through the edges and measured the fluorescence intensity

85 profile on that line (Figure 1E). Indeed, we observed specific fluorescence intensity peaks

86 on the line corresponding to the edges but not at the center (Figure 1F). This observation

87 was further verified by measuring fluorescence intensity around the colony edges and

88 centers which showed significantly high expression at the edge but not at the center cells

89 (Figure 1G). To test if selective transfection of the colony edge cells is a cell type specific

90 phenomenon, we transfected human H9-ESCs and induced pluripotent stem cell (EP1-

91 iPSCs) (Bhise et al., 2013) colonies with CAG-mCherry plasmid. Indeed, we observed

92 increased transfection of the peripheral cells for both the hPSC lines (Figure S1A, S1D).

93 This observation was further verified by measuring fluorescence intensity profiles across

94 the line through the colony center (Figure S1A, S1D) which showed specific intensity

95 peaks at the colony edges but not at the center (Figure S1B, S1E). Similarly, fluorescence

96 intensity measurements showed significantly high fluorescence at the edges compared

97 to centers (Figure S1C, S1F). As hPSCs could be maintained in various media which

98 could affect transfection efficiency, we tested the two most commonly used stem cell

99 media mTeSR1 (mT) and mTeSRplus (mTp) for their effect on hPSC colony transfection

4

100   to further identify the optimum media for transfection. We found significantly higher

101   transfection of H7-ESC colonies when cultured in the mT compared to the mTp media

102   (Figure S2A, S2B) and maintained hPSCs in the mT for this study. However, cellular

103   stemness marker expressions such as OCT4, NANOG, SSEA1, SSEA4, Alkaline

104   Phosphatase (ALPL), SOX2, NOTCH1 and NESTIN did not alter between mT and mTp

105   media (Figure S2C) suggesting stemness property of hPSCs was unaffected when

106   cultured in either media. To test if selective transfection of the colony edge cells is specific

107   to the lipofectamine based transfection, we transduced H7-ESC colonies with the

108   lentivirus containing GFP vector. Interestingly, we observed stem cells throughout the

109   colony got transduced as shown by GFP expression losing the morphological pattern

110   (Figure S3). These data suggest lipofectamine based simple transfection of hPSC

111   colonies selectively transfects edge cells, which could then be isolated to enhance

112   CRISPR genome editing without the need of any viral transduction and antibiotic selection

113   methods.

114

115   **Autophagy driven increased cellular health of hPSC colony edges caused**

116   **increased cell transfection.**

117

118   To investigate the mechanism of selective transfection of hPSC colony edge cells, we

119   asked if cells at the colony edges have more access to the nutrients from the media than

120   the cells at the center, leading to improved cellular health and transfection. Cellular health

121   could be measured by gene expression of the autophagy pathway genes as they get

122   upregulated under stress (Kroemer et al., 2010). Activation of the autophagy pathway

123 genes help by removing damaged proteins and organelles under cellular stress (Anding

124 and Baehrecke, 2017). Hence, we expect cells at the hPSC colony centers will have more

125 autophagy gene expression than the edges. To measure this, we dissected out the H7-

126 hESC cells from the colony edges and centers (Figure 2A) and measured gene

127 expressions for a broad range of autophagy genes (Sha et al., 2018). Indeed, we found

128 key autophagy genes such as ATG5, LC3B, GABARAP, GABARAPL1 and ATG13 are

129 upregulated at the center compared to the edge cells (Figure 2B) suggesting improved

130 cellular health of the edge cells. Of note, the dissected center portion of colony (Figure

131 2A) also contain small portion of edges as dissection of only center cells are extremely

132 difficult and growing colonies very large leads to colony fusions losing edge populations

133 and spontaneous differentiation (Chen et al., 2014). Next, we asked whether the

134 difference in cellular health between colony edge and center affects hPSC stemness

135 property. To test this, we measured stemness marker gene expressions between the

136 edge and center cells of H7-hESC colonies and found no significant difference (Figure

137 2C), suggesting stem cells maintained their stemness property throughout the colony. If

138 stem cells at the colony edges show increased health due to the greater exposure to

139 nutrients leading to more transfection, we asked if creating new edges at the colony center

140 would lead to selective transfection of stem cells at the newly formed edges. To test this,

141 we scratched at the center of H7-hESC colonies to form new edges (Figure S4A) followed

142 by transfection using CAG-mCherry plasmid. Indeed, we observed that cells at the newly

143 formed edges at the former colony center got transfected as shown by the mCherry

144 expression (Figure S4B). Of note, we also have seen some stem cell transfection inside

145 these colony centers (Figure S4B), presumably due to the change in cellular contact upon

146 scratching through the middle of colonies, which is a mechanical perturbation. These

147 suggest that stem cells at the colony centers maintained their stemness as well as the

148 ability to get transfected upon exposure to new edges.

149

150 It has been shown that cells at the hPSC colony edges experience strong myosin II

151 molecular motor mediated contractility of the actin cytoskeleton leading to enhanced

152 contraction of extracellular matrix (ECM) (Närvä et al., 2017; Rosowski et al., 2015). We

153 asked if increased actomyosin contractility at the hPSC colony edges are responsible for

154 selective transfection of these cells. To test this, we inhibited actomyosin contractility by

155 the very potent myosin II ATPase inhibitor blebbistatin (Das et al., 2016) followed by

156 transfection of H7-hESC colonies using CAG-mCherry plasmid. Interestingly, we

157 observed that under myosin II inhibition cells at the edge as well as at the colony center

158 got transfected, losing the edge specific transfection pattern as shown by mCherry

159 expression (Figure 3A). We further observed an overall higher percentage of transfection

160 under myosin II inhibition as measured by flow cytometry (Figure 3B, 3C) which also

161 agrees with the previously reported data (Yen et al., 2014). Myosin inhibition presumably

162 reduced cell-cell contact, making cells more exposed to the transfection reagent and

163 causing cell transfection throughout the colony. Actomyosin contractility leads to the

164 formation of thick F-actin stress fibers within the cells (Tojkander et al., 2012) which we

165 observed in the edge cells of H7-ESC colonies with F-actin stained by fluorescence

166 conjugated phalloidin, indicated by arrows (Figure 3D). We found successful inhibition of

167 actomyosin contractility by blebbistatin as stress fibers disappeared at the hPSC colony

168 edge cells (Figure 3D). Our data showed cells at the hPSC colony centers are under

7

169 stress with increased autophagy gene expressions compared to the edges. We asked if

170 inhibition of the autophagy pathway would increase cellular stress throughout the hPSC

171 colony leading to the inhibition of edge specific cell transfection. To test this, we inhibited

172 the autophagy pathway by using a lysosome inhibitor bafilomycin, followed by CAG-

173 mCherry plasmid transfection. Indeed, we found loss of colony edge specific transfection

174 (Figure 3A) with reduced overall transfection under autophagy inhibition (Figure 3B, 3C)

175 but no loss of F-actin stress fibers at the edge cells was observed (Figure 3D). These

176 data suggest increased cellular health but not the actomyosin contractility of the hPSC

177 colony edge cells is responsible for the selective transfection of those cells.

178

179 **Edge cells at the hPSC colonies showed very high efficiency CRISPR genome**

180 **editing.**

181

182 Finally, we asked if selective transfection of the hPSC colony edge cells could be

183 exploited to have high-efficient CRISPR-Cas9 genome editing. To test this, we

184 transfected H7-hESC colonies using lipofectamine and a plasmid encoding gRNA under

185 U6 promoter and SpCas9-2A-GFP under CAG promoter (Figure 4A). 2A is a non-

186 translatable sequence (Sharma et al., 2012) and after translation, SpCas9 and GFP

187 remain separate without effecting the protein activity. We hypothesized selective

188 transfection of the hPSC colony edge cells would lead to enhanced Cas9 expression in

189 those cells. To test this, we transfected H7-hESC colonies with the above plasmid and

190 dissected out colony edge and center as shown in Figure 4B and measured Cas9

191 expression in the respective populations. Indeed, we observed several fold increased

192   Cas9 expression in edge cells compared to the center (Figure 4C). This is very important

193   as Cas9 delivery followed by gRNA-guided DNA double-strand break (DSB) leads to the

194   insertion-deletions (INDELs) which is the rate-limiting step for obtaining high-frequency

195   genome editing (Hendel et al., 2014, 2015).

196

197   Next, we cloned gRNA into the Cas9 vector (Figure 4A) for mutating hypoxanthine

198   phosphoribosyltransferase 1 (HPRT1). Upon transfection of the H7-hESCs colonies with

199   this plasmid, we observed selective transfection of the cells at the colony edge by GFP

200   expression (Figure 4D) similar to the CAG-mCherry plasmid. gRNA targets a specific

201   gene sequence which allows the Cas9 enzyme to bind and create DNA DSB which cells

202   repair by NHEJ. NHEJ leads to INDELs causing gene mutations. These mutations could

203   be detected by PCR amplifying the DNA sequence around the gRNA target site followed

204   by sanger sequencing and TIDE analysis (Brinkman et al., 2014) of the sequencing data.

205   Since we observed high Cas9 expression in the edge cells, we hypothesized this will lead

206   to high INDEL frequency. Indeed, by TIDE analysis we observed ~38% of edge cells with

207   mutations (62% at 0 INDEL corresponds to 38% mutation) for HPRT1-gene in comparison

208   to the center cells (Figure 4E, F). This is a significant improvement from the reported 3%

209   mutation rate of hPSCs under non-viral and selection free conditions (Yang et al., 2013).

210   This is remarkable as for the first time it allowed us to identify cells from stem cell colonies

211   with very high-frequency genome editing without the need for any viral transduction,

212   FACS sorting or antibiotic selections.

213

214   **DISCUSSION**

215

216   Our work here demonstrated properties of hPSCs within a colony and how that could be

217   used to achieve a selection and viral transduction free CRISPR-Cas9 genome editing

218   technique with very high edit-frequency. This work will have three major impacts on the

219   human disease modeling research; (1) the absence of any antibiotic selection marker will

220   avoid integration of the marker gene and Cas9 into the hPSC genome avoiding unwanted

221   scars or changes, (2) the simple lipofectamine reagent based transfection would allow us

222   to use two or more plasmids with gRNAs targeted for different genes to have double or

223   triple gene knock-out simultaneously, (3) this technique could also be used to create

224   disease causing DNA base pair changes (point mutations) or correct mutations in the

225   patient derived iPSCs by using Cas9 plasmid and single-stranded oligodeoxynucleotides

226   (ssODNs) donor or donor vector. The lipofectamine-stem reagent is compatible for

227   transfecting hPSCs with plasmids as well as ssODNs. Being able to seamlessly edit

228   hPSCs would allow us to differentiate genome edited stem cells to the cell of interest and

229   investigate the human disease mechanism, perform drug screening to identify cell

230   protective agents and replace damaged cells with healthy cells in in-vivo models for cell

231   replacement therapy. This will bring a paradigm shift in the understanding of genotype-

232   phenotype relationship for a variety of human diseases.

233

234   Our data suggested selective transfection of the colony edge cells is due to improved

235   cellular health as revealed by low autophagy gene expressions compared to the center

236   cells (Figure 2). However, it is also possible that the edge cells are more exposed to the

237   transfection reagents than the center leading to increased transfection. This notion could

10

238   be supported by our colony scratch experiment where cells at the new edge in the middle

239   of hPSC colonies got transfected (Figure S4). Our data (Figure 3C) as well as data from

240   another group (Yen et al., 2014) have shown inhibiting actomyosin contractility increased

241   hPSC colony transfection, which could be due to the reduced cell-cell contact within the

242   colony centers exposing cells more to the transfection reagents. Thus, selective

243   transfection of the hPSC colony edge cells could be due to the combination of increased

244   cellular health and more exposure to the transfection reagents.

245

246   **Limitations of Study**

247   This study reveals a very simple but high-efficient genome editing technique in hPSCs

248   with tremendous potential for a broad range of gene editing applications. As a next step,

249   this technique could be used for introducing point mutations in hPSCs or correcting

250   mutations in patient derived iPSCs. Our method here relies on the compact hPSC colony

251   formation to have the distinct edge and center cell population. hPSCs typically grow

252   forming these compact colonies; however if stem cells are grown in non-colony type

253   monolayer (NCM) (Chen et al., 2012) they will not have distinct edge and center cell

254   populations, and hence will limit this method application.

255

256   **ACKNOWLEDGEMENTS**

257

11

260   pluripotent stem cell lines and Drs. Jason Meyer, David Wallace and Timothy Corson for

261   valuable discussions.

262

263   **AUTHOR CONTRIBUTIONS**

264

265   M.S. and A.D. designed the experiments, analyzed data and wrote manuscript; M.S.

266   performed experiments and analyzed data with the help of K.A; A.D. conceived and

267   supervised the project and revised the manuscript.

268

269   **DECLARATION OF INTERESTS**

270

271   The authors declare no competing interests

272

273   **FIGURE LEGENDS**

274   **Figure 1: hESCs selectively got transfected at the colony edges but not at center.**

275   H7-hESCs after clump or single cell passage were transfected with CAG-mCherry (red

276   fluorescence protein, RFP) plasmid and representative brightfield and RFP images were

277   taken 24h after transfection. Shown are images of colony **(A)** and single cells **(B)**. **(C, D)**

278   Transfected cells were dissociated by accutase and run through flow cytometer; shown

279   are the distribution of the RFP-positive cells **(C)** and quantification for percentage of total

280   RFP-positive cells **(D)** with 3 biological repeats for each condition. **(E-F)** Representative

281   images of clump passaged colony 24h after transfection with CAG-mCherry plasmid **(E)**,

282   line trace through the center of colony as shown in (E) shows fluorescence intensity peaks

12

283   at the edges **(F)** but not at the center. **(G)** Quantification of the fluorescence intensity of

284   colony edges and centers from 58 colonies from 5 independent experiments. Error bars

285   are SEM, Student's *t-test*, ∗∗∗, p < 0.0005.

286

287   **Figure 2: hPSCs at the colony edges are healthier with reduced expression of**

288   **autophagy genes.**

289   **(A)** H7-hESCs were cultured and colony edges and centers were dissected for qPCR. **(B,**

290   **C)** qPCR analysis was done on the autophagy genes **(B)** and stemness marker genes

291   **(C)**. ΔΔCt fold changes were measured relative to GAPDH and then to average ΔCt of

292   center. Error bars are SEM, Student's *t-test*, ∗, p-value < 0.05, n=7-15.

293

294   **Figure 3: Inhibiting autophagy but not actomyosin contractility decreases**

295   **transfection efficiency.**

296   **(A)** H7-hESC colonies were treated for 16h with blebbistatin or bafilomycin, then

297   transfected with CAG-mCherry plasmid, shown are images 24h after transfection. **(B, C)**

298   Single cell solutions were collected 24h after transfection and run through flow cytometer,

299   shown are the distribution **(B)** and percentage of RFP-positive cells with-respect-to (w.r.t)

300   control **(C)**. Error bars are SEM, One-way Anova with Dunnett's post hoc; ∗∗, p-value <

301   0.001, n=3. **(D)** Shown are representative confocal immunofluorescence images of F-

302   actin labelled with Alexa Fluor 488 Phalloidin and nucleus labeled with DAPI of H7-hESCs

303   treated for 24h with the indicated drugs. Arrows indicate normal actin stress fiber bundles,

304   n=12.

305

13

306 **Figure 4: Enhanced CRISPR-Cas9 genome editing at the hPSC colony edges.**

307 **(A)** Map of plasmid (Addgene #79144) containing Cas9 and GFP cassettes. (**B, C**) H7-

308 hESCs were transfected with the above plasmid, edges and centers were dissected after

309 24h as shown in **(B)**, and Cas9 expression was measured by qPCR **(C)**. Data presented

310 as ΔCt fold change relative to GAPDH. Error bars are SEM, Student's *t-test*, ∗∗∗, p-value

311 < 0.0005, n=6-9. **(D-F)** HPRT1-gRNA was inserted into the Addgene plasmid and then

312 transfected into H7-hESCs, shown are representative images after 24h of transfection

313 **(D)**. Colony edges and centers were dissected and sequenced for HPRT1 mutation,

314 shown are representative sequencing chromatographs **(E)** and INDEL distribution of edge

315 cells compared to the center cells by TIDE analysis **(F)**, n=12.

316

317 **STAR METHODS**

318

319 **Resource Availability**

320

321 **Lead Contact**

322 Further information and requests for resources and reagents should be directed to

323 Arupratan Das (arupdas@iu.edu)

324

325 **Materials Availability**

326

327 Stem cells and plasmids are available from the Lead Contact's laboratory upon request

328 and completion of the Material Transfer Agreement.

14

329 **Data and Code Availability**

330

331 This study did not generate any code or dataset.

332

333 **EXPERIMENTAL MODEL AND SUBJECT DETAILS:**

334

335 H7-ESCs, H9-ESCs (WiCell, https://www.wicell.org/), and EP1-iPSCs were grown in

336 mTeSR1 media (mT) or mTeSR-plus media (mTp) in 5%CO_2, 37°C incubator on matrigel

337 (MG) coated plates. To obtain hPSC colonies, cells were passaged by clump passaging

338 using Gentle Cell Dissociation Reagent (GD) after reaching 80% confluency. GD was

339 added to cells for 4 min at 37°C, aspirated, then mT was used to resuspend colonies; cell

340 suspension was mixed by pipetting 3-4 times to break up the colonies into small clumps

341 and then seeded into new MG coated wells. Clump passaged colonies were cultured for

342 an additional 2-3 days before experiments. For single cell passaging, cells were incubated

343 with accutase for 10 min and then quenched with double volume of mT with 5 μM

344 blebbistatin. These cells were pelleted by centrifuging at 150G for 5 min, and

345 resuspended in media with blebbistatin, counted, and seeded at a density of 25,000/well

346 of a 24-well plate.

347

348 **METHOD DETAILS**:

349

350 **hPSC transfection**

351

15

352   hPSCs were cultured as described above. The clump passaged colonies using GD were

353   added to a larger volume of media and equally split into the wells of 24-well plates. Single

354   cells after accutase passage were transfected 24h after seeding. GD cells were cultured

355   for another 2-3 days until the colonies were established with distinct edges and centers

356   with colony size around 1/10th the size of a 10x viewscreen at start of drug treatment or

357   transfection. hPSC colonies were treated with 5 μM blebbistatin, 50 nM bafilomycin, or

358   equivalent volume of DMSO in mT for 16h. Cell transfections were done by mixing 2 μl of

359   lipofectamine stem (Invitrogen) and 600 ng of indicated plasmids in 50 μl optimem by

360   vortex. 10 min after vortexing, this mixture was added to the cell culture and incubated

361   for 24h. Images were taken by the EVOS fluorescence microscope (Thermo Fisher

362   Scientific). Using ImageJ software, fluorescence intensity was quantified by drawing a

363   'donut' containing the colony edge, measured as the edge; the 'hole' of the donut was

364   then measured as the center. Raw integrated density was divided by the total area to get

365   the average intensity per area for both edge and center of each colony.

366   **Flow Cytometry**

367   For flow cytometry, cells were incubated in 40 μl accutase for 10 min, then quenched with

368   160 μl mT with 5 μM blebbistatin. This 200 μl cell suspension was transferred into a 96-

369   well round-bottom plate and read on the Attune NxT Acoustic Focusing Flow Cytometer

370   (Thermo) equipped with Attune Auto Sampler (Thermo). Gating was used first to separate

371   live cells, then to separate RFP-positive from the live cell population using the Attune NxT

372   Software. Data were exported to excel or prism for analysis and plotting. Three or more

373   biological repeats were performed for each condition.

374   **qPCR**

16

375   hPSCs were grown in mT and clump passaged using GD. For mT and mTp comparison,

376   H7-hESCs were cultured in the respective media in 6-well plates for more than 2 weeks

377   before starting the experiment. Cells at ~80% confluency were passaged and seeded on

378   24-well MG coated plates for another 4-5 days until they reached ~70% confluency. Cells

379   were incubated with 200 µl accutase for 10 min and resuspended in 400 µl mT with 5 µM

380   blebbistation. Cells were then centrifuged at 150G for 5 min, media aspirated, and cell

381   pellets stored at -20°C. For edge/center comparison, colony dissection was done two

382   days after seeding using clump passaging. When colonies were grown to 1/4 of a 10x

383   field size checked by EVOS, the edge was dissected out first, and then a slice from the

384   center of the colony was collected as the center. Samples were collected into mT with 5

385   µM blebbistatin, with edges and centers from 10 distinct colonies collected into 1

386   biological replicate, with 3 biological replicates total for edge and center. Samples were

387   then centrifuged, media aspirated, and cell pellets stored at -20°C until cDNA preparation.

388   RNA extraction was done following the kit (Qiagen 74104) and 6 µl of RNA was used to

389   prepare cDNA (abm G492). cDNA concentration was measured using Nanodrop 2000c

390   (Thermo) and stored at -80°C. qPCR primers were designed as explained in Table S1.

391   qPCR was performed using Brightgreen (MasterMix-LR, abm) and 100 ng total cDNA in

392   a 20 µl reaction mixture using QuantStudio6 Flex RT PCR system (Applied Biosystems).

393   GAPDH was used as a housekeeping gene in every plate to calculate the ΔCt values.

394   The ΔΔCt was calculated with respect to the average ΔCt of colony center (edge vs.

395   center) or mT (mT vs mTp).

396   **gRNA Cloning**

397   gRNA sequence targeting HPRT1 was obtained from Thermo Fisher (A32060), and then

398   modified following the published protocol (Ran et al., 2013). gRNA was cloned after the

399   U6 promoter sequence into a plasmid containing pCAG-SpCas9-GFP-U6-gRNA

400   (Addgene #79144). 1 μg of plasmid was digested using 1 μl of Bbs1-HF in 1X cutsmart

401   buffer in a total reaction volume of 50 μl. This was then run in 1% agarose gel, and gel

402   extracted following the kit (Zymo D4007).

403   10 μM of sense and antisense gRNA oligos were added to 1X T4 DNA ligase reaction

404   buffer with 0.5 μl of T4 Polynucleotide Kinase for a final volume of 10 μl and annealed in

405   the thermocycler (37°C for 30 min, then 95°C for 5 min, and ramp down to 25°C at

406   5°C/min). The annealed gRNA was ligated into the gel extracted plasmid by adding 50 μg

407   of the Bbs1-HF digested plasmid, 1 μl of annealed oligo duplex, and 5 μl of 2x quick

408   ligation buffer for a final volume of 10 μl. 1 μl of quick ligase was then added and the

409   reaction incubated at room temperature for 10 min. 2 μl of this plasmid was added to 50

410   μl of Top10 *E coli* and kept in ice for 5 min. The bacteria were then heat shocked to

411   promote uptake of the plasmid at 42°C for 45 seconds before being placed back into ice

412   for 2 min. 250 μl SOC media was added to the bacteria and incubated in a 37°C shaker

413   for 1h before being spread onto LB-agar plates with Carbenicillin (50 μg/ml) and incubated

414   overnight at 37°C. The next day, colonies were picked and grown into LB-broth with

415   Carbenicillin overnight at 37°C under shaking. Plasmid was extracted following the kit

416   (Zymo D4210), and concentration was measured using nanodrop. Plasmids were

417   sequenced by Eurofins to check gRNA integration.

418   **Confocal Imaging**

419   hPSCs were seeded using GD passaging on MG-coated glass bottom dishes (MatTek).

420   The next day, 5μM blebbistatin, 50 nM bafilomycin, or equivalent volume of DMSO was

421   added to the culture media for 24h. Media was aspirated and cells were washed with 1X

422   PBS, and then fixed with 4% Paraformaldehyde for 30 min at 37°C. Cells were washed

423   once and then stored in PBS at 4°C until immunostained. Fixed cells were permeabilized

424   with 0.5% Triton-X100 in PBS for 5 min and then washed in PBST (1X PBS + 0.1%

425   Tween20) for 3 times for 5 minutes each. Cells were blocked with PBS containing 5%

426   donkey serum and 0.1% Tween 20 (blocking buffer). Alexa Fluor 488 conjugated

427   Phalloidin (4U/ml) was added to the blocking buffer and incubated with the cells for 1h in

428   the dark at room temperature. Dishes were washed with 1X PBST 3 times for 5 minutes

429   each, with 1.43 μM DAPI added to the second wash. Cells were stored in 1x PBS while

430   being imaged on Zeiss LSM700 with 63x/1.4 oil objective. Analysis was done using

431   ImageJ with maximum projections of DAPI channel and the middle confocal slice of the

432   Phalloidin labelled F-actin channel of the z-stacks.

433   **CRISPR-Cas9 genome editing of hESCs**

434   H7-hESC colonies were grown and transfected with the plasmid containing HPRT1-gRNA

435   and Cas9 (gRNA cloning protocol) using 600 ng of plasmid with 50 μl optimem and 2 μl

436   lipofectamine stem (Invitrogen). Colony dissection was performed 24h after transfection;

437   edge and center samples were collected and plated into mT with 5 μM blebbistatin in a

438   96 well MG-coated plate, with each colony piece in its own well. After 24h, media was

439   changed to mT without blebbistatin, with culture continuing for another 7-10 days with mT

440   changed daily. After cells had grown sufficiently, media was aspirated and 30 μl of quick

441   extraction buffer was added to each well and a pipet was used to mix and scrape any

19

442   cells from the plate and transfer them into PCR tubes. Samples were then vortexed, spun

443   down, and heated at 65°C for 10 min followed by 95°C for 5 min to extract DNA. After

444   which the concentration was measured on a nanodrop and 50-200 ng of DNA was used

445   with Phusion-Flash mastermix to PCR amplify the DNA sequence around the HPRT1

446   gRNA target site. The PCR product was run in 1.5% agarose gel with Ethidium Bromide,

447   and gel extracted following the kit (Zymo D4007). Extracted DNA was then sent for

448   sequencing with Eurofins and analyzed with TIDE analysis software (https://tide.nki.nl/)

449   where CRISPR edge samples were compared to the respective centers.

450

Lentivirus

452   H7-hESCs at ~80% confluency were clump passaged using GD and seeded into 96-well

453   MG coated wells. The next day, cell counting was done from a well using accutase

454   mediated single cell dissociation. Lentivirus (LV) (Life Technologies Cat # A32060) with

455   viral vector containing P_{U6}-HPRT1(gRNA)-P_{EFS}-GFP was added at multiplicity of infection

456   (MOI) of 10 for each well. LV was added through mT media containing 8 μg/mL polybrene

457   and the plate was centrifuged at 800 G at room temperature for 1h before incubating at

458   37°C, 5% CO_2 incubator overnight. The next day, media with lentivirus was removed and

459   replaced with normal mT; mT was changed every following day and GFP signal was

460   observed over time.

Quantification and Statistical analysis:

462

463   All data presented are mean ± SEM. For statistical analysis between two independent

464   conditions a Student's *t-test* was performed in Microsoft Excel; for more than two

465   conditions, one-way Anova with Dunnett's multiple comparison post hoc test was

466   performed using GraphPad Prism 9.0 software.

467

468   **REFERENCES**

469

470   Anding, A.L., and Baehrecke, E.H. (2017). Cleaning House: Selective Autophagy of

471   Organelles. Dev. Cell *41*, 10–22.

472   Bhise, N.S., Wahlin, K.J., Zack, D.J., and Green, J.J. (2013). Evaluating the potential of

473   poly(beta-amino ester) nanoparticles for reprogramming human fibroblasts to become

474   induced pluripotent stem cells. Int. J. Nanomedicine *8*, 4641–4658.

475   Brinkman, E.K., Chen, T., Amendola, M., and Van Steensel, B. (2014). Easy

476   quantitative assessment of genome editing by sequence trace decomposition. Nucleic

477   Acids Res. *42*.

478   Byrne, S.M., and Church, G.M. (2015). CRISPR-mediated gene targeting of human

479   induced pluripotent stem cells. Curr. Protoc. Stem Cell Biol. *2015*, 5A.8.1-5A.8.22.

480   Chen, K.G., Mallon, B.S., Hamilton, R.S., Kozhich, O.A., Park, K., Hoeppner, D.J.,

481   Robey, P.G., and McKay, R.D.G. (2012). Non-colony type monolayer culture of human

482   embryonic stem cells. Stem Cell Res. *9*, 237–248.

483   Chen, K.G., Mallon, B.S., McKay, R.D.G., and Robey, P.G. (2014). Human pluripotent

484   stem cell culture: Considerations for maintenance, expansion, and therapeutics. Cell

485   Stem Cell *14*, 13–26.

486   Das, A., Fischer, R.S., Pan, D., and Waterman, C.M. (2016). YAP nuclear localization in

487   the absence of cell-cell contact is mediated by a filamentous actin-dependent, Myosin

488 IIand Phospho-YAP-independent pathway during extracellular matrix mechanosensing.

489 J. Biol. Chem. *291*, 6096–6110.

490 Ding, Q., Regan, S.N., Xia, Y., Oostrom, L.A., Cowan, C.A., and Musunuru, K. (2013).

491 Enhanced efficiency of human pluripotent stem cell genome editing through replacing

492 TALENs with CRISPRs. Cell Stem Cell *12*, 393–394.

493 Hendel, A., Kildebeck, E.J., Fine, E.J., Clark, J.T., Punjya, N., Sebastiano, V., Bao, G.,

494 and Porteus, M.H. (2014). Quantifying genome-editing outcomes at endogenous loci

495 with SMRT sequencing. Cell Rep. *7*, 293–305.

496 Hendel, A., Bak, R.O., Clark, J.T., Kennedy, A.B., Ryan, D.E., Roy, S., Steinfeld, I.,

497 Lunstad, B.D., Kaiser, R.J., Wilkens, A.B., et al. (2015). Chemically modified guide

498 RNAs enhance CRISPR-Cas genome editing in human primary cells. Nat. Biotechnol.

499 *33*, 985–989.

500 Kroemer, G., Mariño, G., and Levine, B. (2010). Autophagy and the Integrated Stress

501 Response. Mol. Cell *40*, 280–293.

502 Lombardo, A., Genovese, P., Beausejour, C.M., Colleoni, S., Lee, Y.L., Kim, K.A.,

503 Ando, D., Urnov, F.D., Galli, C., Gregory, P.D., et al. (2007). Gene editing in human

504 stem cells using zinc finger nucleases and integrase-defective lentiviral vector delivery.

505 Nat. Biotechnol. *25*, 1298–1306.

506 Martin, R.M., Ikeda, K., Cromer, M.K., Uchida, N., Nishimura, T., Romano, R., Tong,

507 A.J., Lemgart, V.T., Camarena, J., Pavel-Dinu, M., et al. (2019). Highly Efficient and

508 Marker-free Genome Editing of Human Pluripotent Stem Cells by CRISPR-Cas9 RNP

509 and AAV6 Donor-Mediated Homologous Recombination. Cell Stem Cell *24*, 821-828.e5.

510 Mignon, C., Sodoyer, R., and Werle, B. (2015). Antibiotic-free selection in

22

511   biotherapeutics: Now and forever. Pathogens *4*, 157–181.

512   Närvä, E., Stubb, A., Guzmán, C., Blomqvist, M., Balboa, D., Lerche, M., Saari, M.,

513   Otonkoski, T., and Ivaska, J. (2017). A Strong Contractile Actin Fence and Large

514   Adhesions Direct Human Pluripotent Colony Morphology and Adhesion. Stem Cell

515   Reports *9*, 67–76.

516   Ran, F.A., Hsu, P.D., Wright, J., Agarwala, V., Scott, D.A., and Zhang, F. (2013).

517   Genome engineering using the CRISPR-Cas9 system. Nat. Protoc. *8*, 2281–2308.

518   Rosowski, K.A., Mertz, A.F., Norcross, S., Dufresne, E.R., and Horsley, V. (2015).

519   Edges of human embryonic stem cell colonies display distinct mechanical properties

520   and differentiation potential. Sci. Rep. *5*.

521   Saha, K., and Jaenisch, R. (2009). Technical Challenges in Using Human Induced

522   Pluripotent Stem Cells to Model Disease. Cell Stem Cell *5*, 584–595.

523   Sha, Z., Schnell, H.M., Ruoff, K., and Goldberg, A. (2018). Rapid induction of p62 and

524   GAB ARA PL1 upon proteasome inhibition promotes survival before autophagy

525   activation. J. Cell Biol. *217*, 1757–1776.

526   Sharma, P., Yan, F., Doronina, V.A., Escuin-Ordinas, H., Ryan, M.D., and Brown, J.D.

527   (2012). 2A peptides provide distinct solutions to driving stop-carry on translational

528   recoding. Nucleic Acids Res. *40*, 3143–3151.

529   Sluch, V.M., Chamling, X., Wenger, C., Duan, Y., Rice, D.S., and Zack, D.J. (2018).

530   Highly efficient scarless knock-in of reporter genes into human and mouse pluripotent

531   stem cells via transient antibiotic selection. PLoS One *13*.

532   Steyer, B., Bu, Q., Cory, E., Jiang, K., Duong, S., Sinha, D., Steltzer, S., Gamm, D.,

533   Chang, Q., and Saha, K. (2018). Scarless Genome Editing of Human Pluripotent Stem

534   Cells via Transient Puromycin Selection. Stem Cell Reports *10*, 642–654.

535   Tojkander, S., Gateva, G., and Lappalainen, P. (2012). Actin stress fibers - Assembly,

536   dynamics and biological roles. J. Cell Sci. *125*, 1855–1864.

537   Vandermeulen, G., Marie, C., Scherman, D., and Préat, V. (2011). New generation of

538   plasmid backbones devoid of antibiotic resistance marker for gene therapy trials. Mol.

539   Ther. *19*, 1942–1949.

540   Yang, L., Guell, M., Byrne, S., Yang, J.L., De Los Angeles, A., Mali, P., Aach, J., Kim-

541   Kiselak, C., Briggs, A.W., Rios, X., et al. (2013). Optimization of scarless human stem

542   cell genome editing. Nucleic Acids Res. *41*, 9049–9061.

543   Yen, J., Yin, L., and Cheng, J. (2014). Enhanced non-viral gene delivery to human

544   embryonic stem cells via small molecule-mediated transient alteration of the cell

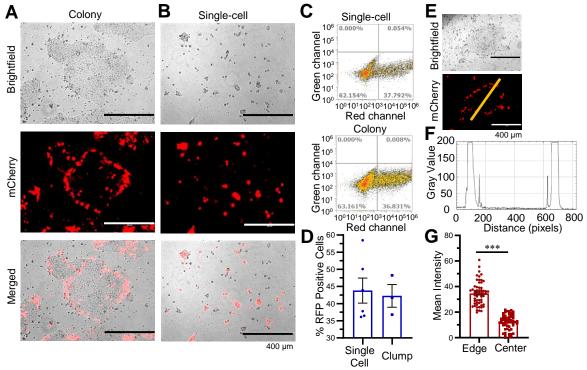545   structure. J. Mater. Chem. B *2*, 8098–8105.

546

Figure 1. hESCs selectively get transfected at the colony edges but not center.
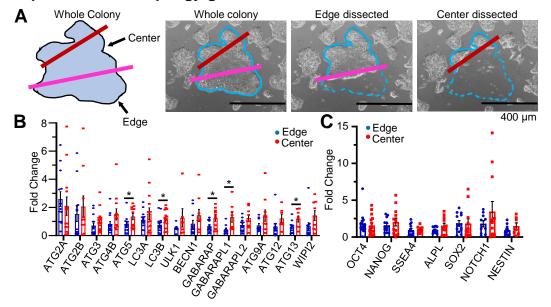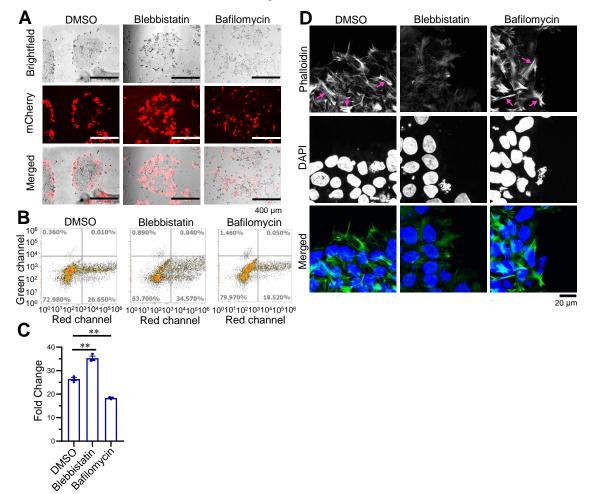
Figure 2. hPSCs at the colony edges are healthier with reduced expression of autophagy genes.

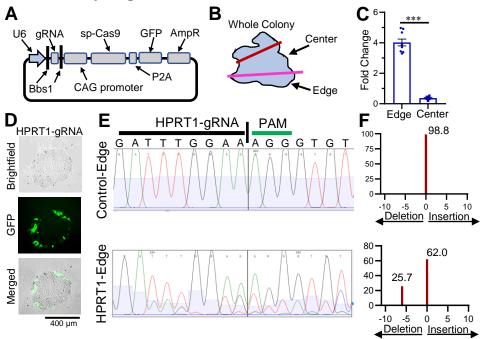**Figure 3. Inhibiting autophagy but not actomyosin contractility decreases transfection efficiency.**

Figure 4. Enhanced CRISPR-Cas9 genome editing at the hPSC colony edges.

KEY RESOURCES TABLE

REAGENT or RESOURCE	SOURCE	IDENTIFIER
Antibodies		
Alexa Fluor 488 Phalloidin	Invitrogen	Cat# A12379
Bacterial and Virus Strains		
Invitrogen™ One Shot™ TOP10 Chemically Competent *E. coli*	Fisher Scientific	Cat# C404003
Chemicals, Peptides, and Recombinant Proteins		
Matrigel	Corning	Cat# CB40230
Gentle Cell Dissociation Reagent	Stem Cell Technology	Cat# 7174
mTeSR1	Stem Cell Technology	Cat# 85850
mTeSR-Plus	Stem Cell Technololgy	Cat# 5825
Accutase	Sigma	Cat# A6964
Blebbistatin	Sigma	Cat# B0560
Bafilomycin	Sigma	Cat# B1793
DAPI	Molecular Probes	Cat# D1206
DMSO	Sigma	Cat# 276855
Lipofectamine Stem	Invitrogen	Cat# STEM00003
Optimem	Gibco	Cat# 31985070
Parafomaldehyde 16% solution, EM grade	Electron Microscopy Sciences	Cat# 15710
Triton-X-100	Sigma	Cat# T8787
Donkey Serum	Sigma	Cat# D9663
Tween-20	Sigma	Cat# P9416
Polybrene	Sigma	Cat# TR-1003-G
Bbs1-HF	New England BioLabs	Cat# R3539S
Cutsmart Buffer	New England BioLabs	Cat# B7204S
T4 DNA Ligase Reaction Buffer	New England BioLabs	Cat# B0202S
T4 Polynucleotide Kinase (PNK)	New England BioLabs	Cat# M0201S
Quick Ligation Buffer	New England BioLabs	Cat# B2200
Quick Ligase	New England BioLabs	Cat# M2200S
SOC media	Fisher Scientific	Cat# BP974010X5
Carbenicillin	Sigma	Cat# C1389
LB Broth (Miller)	Sigma	Cat# L3522
LB broth with agar (Miller)	Sigma	Cat# L3147
Quick Extraction Buffer	Epicentre	Cat# QE09050
Phusion Flash Mastermix	Fisher Scientific	Cat# F548L
Agarose	Sigma	Cat# A9539
Ethidium Bromide	Sigma	Cat# E1510
Critical Commercial Assays		
RNeasy Mini Kit	Qiagen	Cat# 74104
5x all-in-one RT MasterMix (with AccuRTGenomic DNA Removal kit)	applied biological materials	Cat# G492
BrightGreen 2x qPCR MasterMix-Low ROX	applied biological materials	Cat# MasterMix-LR
ZymoPURE™ Plasmid Miniprep Kit	Zymo	Cat# D4210
Zymoclean Gel DNA Recovery Kit	Zymo	Cat# D4007

Experimental Models: Cell Lines		
H7-hESCs, H9-hESCs	WiCell; Sluch et al., 2018	
EP1-iPSCs	Bhise et al., 2013	
Oligonucleotides		
HPRT1-gRNA-Forward	ThermoFisher website; alterations following Ran et al., 2013	CACCGATTATGCTGAGGATTTGGAA
HPRT1-gRNA-Reverse	ThermoFisher website; alterations following Ran et al., 2013	AAACTTCCAAATCCTCAGCATAATC
gRNA plasmid sequencing		CGCCAGCAACGCGGCCTTTTTACGG
HPRT1-PCR-Forward; sequencing	ThermoFisher website	TACACGTGTGAACCAACCCG
HPRT1-PCR-Reverse	ThermoFisher website	GTAAGGCCCTCCTCTTTTATTT
Primers for qPCR	Supplemental Table S1	
Recombinant DNA		
pCAG-mCherry plasmid	Addgene	Cat# 108685
pCAG-SpCas9-P2A-GFP-U6-gRNA	Addgene	Cat# 79144
pCAG-SpCas9-P2A-GFP-U6-HPRT1	This paper	N/A
LentiArray™ CRISPR Positive Control Lentivirus, human HPRT, with GFP (P_{U6}-HPRT1-P_{EFS}-GFP)	ThermoFisher (Life Technologies)	Cat# A32060
Software and Algorithms		
ImageJ	NIH	
Attune NxT Software	ThermoFisher	
Prism version 9	GraphPad	
Zen Microscope Software	Zeiss	
Genescript	https://www.genscript.com/	
Primer3	https://primer3.ut.ee/	
PrimerBank	https://pga.mgh.harvard.edu/primerbank/	
TIDE analysis software	https://tide.nki.nl/	